CONF-8410256--3

CONF-8410256--3

DE86 002268

BACKGROUND INFORMATION ON NEUTRON FLUX FOR AN ADVANCED HIGH-FLUX REACTOR

R. M. Moon

Solid State Division
Oak Ridge National Laboratory
Oak Ridge, Tennessee 37831
operated by
Martin Marietta Energy Systems, Inc.
for the
U.S. Department of Energy
under Contract No. DE-AC05-840R21400

January 1985

BACKGROUND INFORMATION ON NEUTRON FLUX FOR AN ADVANCED HIGH-FLUX REACTOR

R. M. Moon, Oak Ridge National Laboratory

I. SOURCE FLUX

We assume a large D_2O reflector equipped with cold source(s), a hot source, and with a peak thermal flux in the reflector of $\phi_0 = 5 \times 10^{15}$ n cm^{-2} sec^{-1}. In this section we estimate the flux distributions $\frac{d^2\phi}{d\Omega d\lambda}$ (n cm^{-2} sec^{-1} sterad^{-1} Å^{-1}) for thermal, cold, and hot beams.

A. Thermal Distribution

We assume an isotropic, Maxwell-Boltzmann distribution.

$$\frac{d^2\phi}{d\Omega d\lambda} = \frac{\phi_0}{4\pi} \nu_\lambda(T_0,\lambda) \tag{1}$$

$$\nu_\lambda(T_0,\lambda) = \frac{2}{\lambda}\left(\frac{E}{E_0}\right)^2 e^{-E/E_0} = 2\,\lambda_0^4\,\lambda^{-5}\,e^{-(\lambda_0/\lambda)^2} \tag{2}$$

$$\lambda_0[\text{Å}] = 30.81/\sqrt{T_0[^\circ\text{K}]} \tag{3}$$

$$E_0[\text{meV}] = 0.08616\ T_0[^\circ\text{K}] \tag{4}$$

Figure 1 shows a comparison between the observed distribution at the H12 thermal beam[1] at the ILL and a calculated distribution with $\phi_0 = 1.2 \times 10^{15}$ n cm^{-2} sec^{-1} and $T_0 = 310$ K. These parameters give a fairly good agreement, particularly for $\lambda > 0.9$ Å. Accordingly, to describe the thermal spectrum at our assumed reactor, we use $\phi_0 = 5 \times 10^{15}$ and $T_0 = 310$ K.

If it is desired to express the distribution in terms of an energy interval, the appropriate equations are

$$\frac{d^2\phi}{d\Omega dE} = \frac{\phi_0}{4\pi} \nu_E\ (T_0,E)\ , \tag{5}$$

$$\nu_E(T_0,E) = \frac{E}{E_0^2} e^{-E/E_0} \quad . \tag{6}$$

Note that

$$\int_0^\infty \nu_\lambda \, d\lambda = \int_0^\infty \nu_E \, dE = 1 \ , \tag{7}$$

and that

$$\nu_\lambda = \frac{2E}{\lambda} \nu_E \ , \tag{8}$$

and that

$$\lambda[\text{Å}] = \frac{9.044}{\sqrt{E[\text{meV}]}} \quad . \tag{9}$$

B. Cold Distribution

The problem with cold source spectra is that they do not follow a Maxwell-Boltzmann distribution, as pointed out by Ageron et al.[2] Therefore, in estimating the cold neutron spectrum for our 5 x 10^{15} reactor we will rely on a scaled-up version of the ILL distribution. There is even a problem with this procedure in that the calculated ILL cold source spectrum[3,4] is significantly higher than that derived from neutron guide measurements.[1] This difference is now completely understood by Ageron[5] and is due to three effects: (1) the original calculation was based on unperturbed rather than the perturbed flux at the cold source position, (2) the calculation was based on gain factors measured with a larger D_2 volume than that in the HFR installation, and (3) the real guide transmission is not perfect. Recent calculations are in excellent agreement with the measured guide spectra.

According to Ageron[3], the unperturbed thermal flux at the cold source position is $(4\pi)(3)10^{13}$ = 3.8 x 10^{14} n cm^{-2} sec^{-1}. We hope to install a cold source in a region with unpertubed thermal flux of 2–3 x 10^{15} n cm^{-2} sec^{-1}, so it is reasonable to use a scale factor of six applied to the ILL spectrum in making this estimate. The upper curve marked "cold A" in Fig. 2

is based on the original ILL calculation[3,4] and the lower "cold B" curve is based on the measured guide spectra, assuming perfect guide transmission. If our purpose is a comparison with the pulsed source described by Crawford et al. in these proceedings, then the "cold A" curve should be used because they have also used this curve in generating the cold source spectrum for the case of a liquid D_2 source embedded in a large D_2O moderator. If our purpose is to compare with existing ILL instruments, then probably the "cold B" curve should be used. By changing the shape of the ILL cold source, Ageron estimates that the cold flux can be increased by a factor of 1.8. This "reentrant factor" has not been included in the curves of Fig. 2.

C. Hot Distribution

We base our hot source distribution of Fig. 2 on the H3 curve of Ref. 1 using a scale factor of four to go from a 1.2×10^{15} reactor to a 5×10^{15} reactor.

D. Summary

The hot, thermal, and cold distributions are given in Fig. 2. The hot distribution is based on the H3 curve of Ref. 1 with a scale factor of four. The thermal distribution is based on Eqs. (1), (2), and (3) with $T_0 = 310$ K and $\phi_0 = 5 \times 10^{15}$ n/cm^2 sec. The cold distributions are based on the ILL cold source with a scale factor of six. For comparison with the "state-of-the-art" pulsed source with a large D_2O moderator and a D_2 cold source, the curve labeled "cold A" should be used.

II. BEAM TUBES, GUIDES, AND MONOCHROMATOR SYSTEMS

In this section we summarize equations needed to calculate neutron intensities delivered by beam tubes and guides and present some expected intensities for the assumed 5×10^{15} reactor. In addition, the equations needed to calculate monochromatic intensities delivered to the sample by a crystal monochromator are presented.

A. Beam Tubes and Guides

$$I(\lambda) = \phi''(\lambda)\delta_H(\lambda)\delta_V(\lambda) \quad [\text{n cm}^{-2}\ \text{sec}^{-1}\ \text{Å}^{-1}] \tag{10}$$

where $\phi'' = d^2\phi/d\Omega d\lambda$ and δ_H and δ_V are the horizontal and vertical angular divergences of the tube or guide.

Beam Tube

For a beam tube of width w_S and height h_S at the source and of length L_O, we have

$$\delta_H = w_S/L_O \tag{11}$$

$$\delta_V = h_S/L_O. \tag{12}$$

Typical values might be w_S = 10 cm, h_S = 15 cm, and L_O = 700 cm.

Straight Guide (Long)

$$\delta_H = \delta_V = 2\theta_C = 2\ K\ \lambda\ . \tag{13}$$

The constant K is listed below for various guide coating materials.

	K (radians Å^{-1})
Ni	$1.73\ 10^{-3}$
^{58}Ni	$2.05\ 10^{-3}$
Supermirror	$3.81\ 10^{-3}$

Horizontally Bent Guide

The result of Maier-Leibnitz and Springer[6] can be written as follows,

$$\delta_V = 2\ K\ \lambda \tag{14}$$

$$\delta_H = \left(\frac{\bar{\omega}}{\omega_S}\right)\delta_V \tag{15}$$

$$\left(\frac{\bar{\omega}}{\omega_S}\right) = \begin{cases} \frac{2}{3}\left(\frac{\lambda}{\lambda^*}\right)^2 \left[1 - \left(1 - \left(\frac{\lambda^*}{\lambda}\right)^2\right)^{3/2}\right] & \text{for } \frac{\lambda}{\lambda^*} > 1 \\ \frac{2}{3}\left(\frac{\lambda}{\lambda^*}\right)^2 & \text{for } \frac{\lambda}{\lambda^*} < 1. \end{cases} \quad (16)$$

λ^* is the cut-off wavelength given by

$$\lambda^* = \frac{1}{K}\sqrt{2d/\rho} \quad , \quad (17)$$

where d is the guide width and ρ the radius of curvature. The dimensionless function $(\bar{\omega}/\omega_S)$, which is the ratio of the average solid angle for the bent guide to that of a straight guide of identical reflecting material is plotted in Fig. 3. Note that this depends only on (λ/λ^*) and so can be used for any reflecting material and any radius of curvature.

The above equations have been used, in combination with the source spectral distributions of Fig. 2, to calculate the intensities delivered by various beam tubes and guides. The results are shown in Fig. 4 and the associated angular divergences are shown in Fig. 5. Note that the cold guide curves are for the usual Ni coating and are based on the "cold A" curve of Fig. 2. These intensities and angular divergences can be converted to ^{58}Ni by multiplying by 1.4 and to the supermirror case by multiplying by 4.8.

B. Intensity at Sample - Crystal Monochromator

We start with the usual Cooper and Nathans probability function (horizontal part only).

$$P_H(\Delta\lambda, \gamma_1) = P_M \exp\left\{-\frac{1}{2}\left[\left(\frac{\gamma_1 - (\Delta\lambda/\lambda)\tan\theta_M}{\eta_M}\right)^2 + \left(\frac{\gamma_1 - 2(\Delta\lambda/\lambda)\tan\theta_M}{\alpha_0}\right)^2 + \left(\frac{\gamma_1}{\alpha_1}\right)^2\right]\right\}. \quad (18)$$

The intensity on the sample is given by

$$I(\lambda) = \phi''(\lambda)\ \delta\gamma \int_{-\infty}^{+\infty} P_H(\Delta\lambda, \gamma_1)\ d\Delta\lambda\ d\gamma_1\ [n\ cm^{-2}\ sec^{-1}]\ . \tag{19}$$

The vertical divergence for a flat monochromator is

$$\delta\gamma = \frac{h_S}{L_0 + L_1}\ , \tag{20}$$

where h_S is the source height, L_0 is the source to monochromator distance, and L_1 is the monochromator to sample distance. For a vertically focused monochromator[7]

$$\delta\gamma = \frac{h_M}{L_1}\ , \tag{21}$$

where h_M is the monochromator height. Performing the integrations in Eq. (19), we obtain

$$I(\lambda) = \phi''(\lambda)\ P_M(\lambda)\delta\gamma\ \lambda\ \cot\theta_M \frac{2\pi}{8\ell n2}\ \frac{\bar{\alpha}_0\ \bar{\alpha}_1\ \bar{\eta}_M}{\sqrt{\bar{\alpha}_0^2 + \bar{\alpha}_1^2 + 4\bar{\eta}_M^2}}\ , \tag{22}$$

where the width parameters have been converted to FWHM values,

$$\bar{\alpha}_i = 2\sqrt{2\ell n2}\ c_i,\ \text{etc.} \tag{23}$$

The factor $P_M(\lambda)$ is the peak absolute reflectivity of the crystal and the numerical factor $2\pi/8\ell n2$ is equal to 1.13. The FWHM in the wavelength distribution of neutrons incident on the sample, obtained by integrating Eq. (18) over γ_1, is

$$\frac{\Delta\lambda}{\lambda} = \frac{1}{2}\ \frac{\Delta E}{E} = \cot\theta_M \left(\frac{\bar{\alpha}_0^2\ \bar{\alpha}_1^2 + \bar{\alpha}_0^2\ \bar{\eta}_M^2 + \bar{\alpha}_1^2\ \bar{\eta}_M^2}{\bar{\alpha}_0^2 + \bar{\alpha}_1^2 + 4\bar{\eta}_M^2} \right)^{1/2} \tag{24}$$

Similarly the horizontal divergence (FWHM), obtained by integrating Eq. (18) over $\Delta\lambda$, is

$$\Delta\gamma_1 = \alpha_1 \left[\frac{\bar{\alpha}_0^2 + 4\bar{\eta}_M^2}{\bar{\alpha}_1^2 + \bar{\alpha}_0^2 + 4\bar{\eta}_M^2} \right]^{1/2} . \tag{25}$$

Note that for the special case $\alpha_0 = \alpha_1 = \eta_M$,

$$I(\lambda) = \phi''(\lambda)\, P_M(\lambda)\, \delta_V\, \lambda \cot\theta_M (1.13) \frac{\bar{\eta}_M^2}{\sqrt{6}} \tag{26}$$

$$\frac{\Delta\lambda}{\lambda} = \cot\theta_M \frac{\bar{\eta}_M}{\sqrt{2}} \tag{27}$$

$$\Delta\gamma_1 = \alpha_1 \sqrt{5/6} . \tag{28}$$

Another interesting case is $\alpha_0 \gg \alpha_1 = \eta_M$, for which

$$I(\lambda) = \phi''(\lambda)\, P_M(\lambda)\, \delta_V\, \lambda \cot\theta_M (1.13)\, \bar{\eta}_M^2 \tag{29}$$

$$\frac{\Delta\lambda}{\lambda} = \cot\theta_M\, \bar{\eta}_M \sqrt{2} \tag{30}$$

$$\Delta\gamma_1 = \bar{\alpha}_1 . \tag{31}$$

In cases where Soller collimators are not used before the monochromator, the value of α_0 can be taken as the horizontal divergence of the tube or guide discussed previously.

III. COMPARISON WITH PULSED-SOURCE SPECTRA

The connection between I(E) plotted in Fig. 1 of the notes by Crawford, Russell and Carpenter and $d^2\phi/d\Omega d\lambda$ plotted in my Fig. 2 is apparent by

observing that, in their notation,

$$\phi(E) = \frac{I(E)}{L^2} = \frac{I(E)}{A_{Mod}} \frac{A_{Mod}}{L^2} = \frac{I(E)}{A_{Mod}} \delta_H \delta_V \cdot$$

So their quantity $I(E)/A_{Mod}$ is equivalent to my $d^2\phi/d\Omega dE$. Since they have used $A_{Mod} = 100$ cm^2 the I(E) values of their Fig. 1 should be multiplied by 10^{-2} to compare with my $d^2d/d\Omega dE$. The comparison with the time-averaged pulsed source spectra is shown in Fig. 6 after converting my wavelength distributions of Fig. 2 to energy distributions by multiplying by $\lambda/2E$.

REFERENCES

1. "Neutron Beam Facilities Available for Users," ILL, Jan. 1981.
2. P. Ageron, Ph. De Beaucourt, H. D. Harig, A. Locaze, and M. Livolant, Cryogenics, February (1969).
3. P. Ageron, R. Ewald, H. D. Harig, and J. Verdier, Energie Nucleaire 13, 1 (1971).
4. P. Ageron, Bulletin d'Informations Scientifiques et Techniques 166, 5 (1972).
5. P. Ageron (private communcation).
6. H. Maier-Leibnitz and T. Springer, Reactor Science and Technology 17, 217 (1963).
7. R. Currat, Nuclear Instr. and Meth. 107, 21 (1973).

FIGURE CAPTIONS

Fig. 1. Calculated thermal distribution compared to H12 beam tube, ILL.

Fig. 2. Estimated flux distributions for 5×10^{15} reactor.

Fig. 3. Bent guide cut-off function.

Fig. 4. Spectral distributions of various beams from a 5×10^{15} reactor.

Fig. 5. Angular divergence of tubes and guides of Fig. 4.

Fig. 6. Comparison of source spectra for 5×10^{15} reactor and state-of-the-art pulsed source.

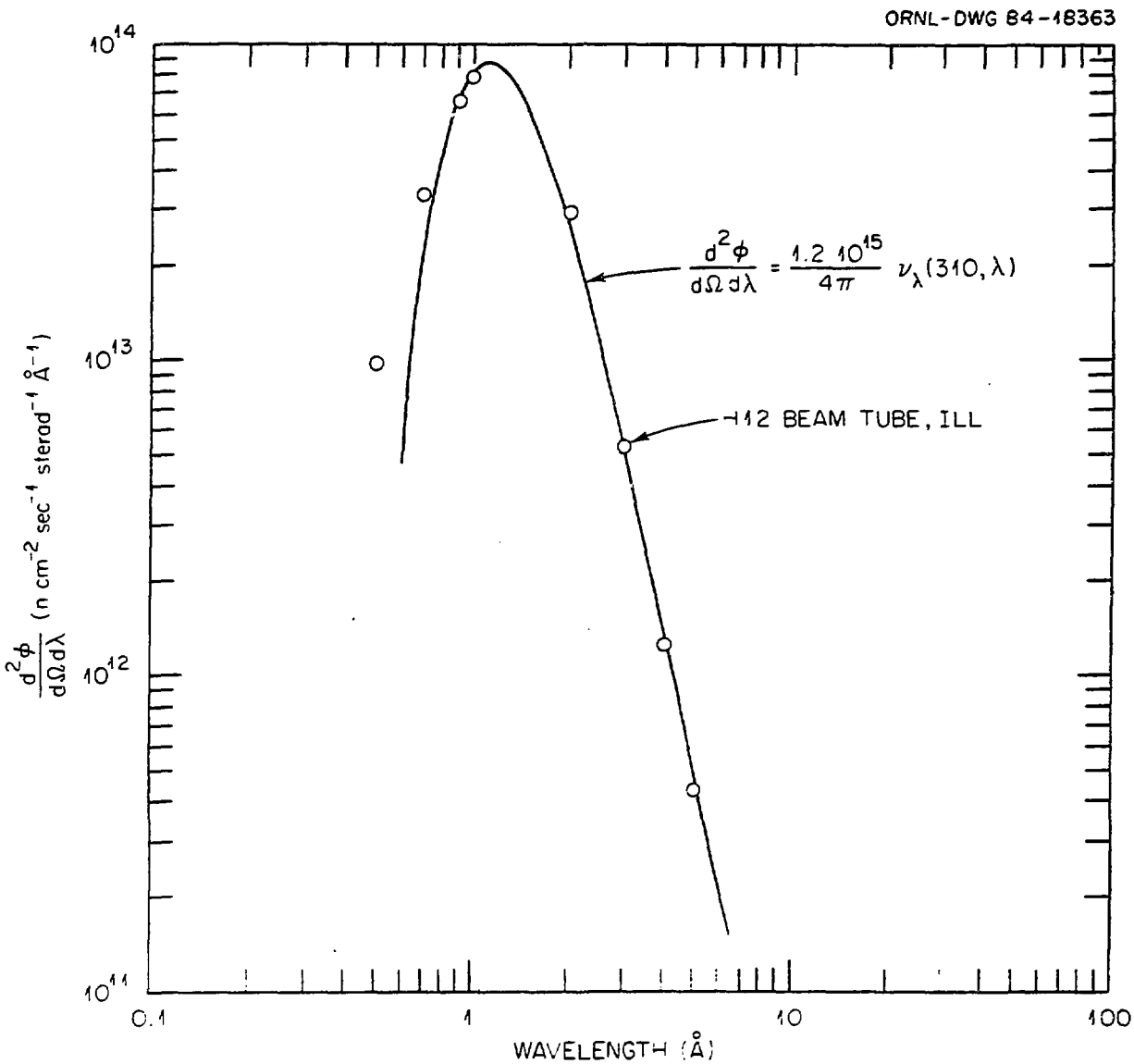
ORNL-DWG 84-18363
10^{14}
10^{13}
10^{12}
10^{11}
$\frac{d^2\phi}{d\Omega\, d\lambda}$ (n cm^{-2} sec^{-1} sterad^{-1} Å^{-1})
$\frac{d^2\phi}{d\Omega\, d\lambda} = \frac{1.2\ 10^{15}}{4\pi}\ \nu_\lambda(310, \lambda)$
H12 BEAM TUBE, ILL
0.1
1
10
100
WAVELENGTH (Å)

Fig. 1

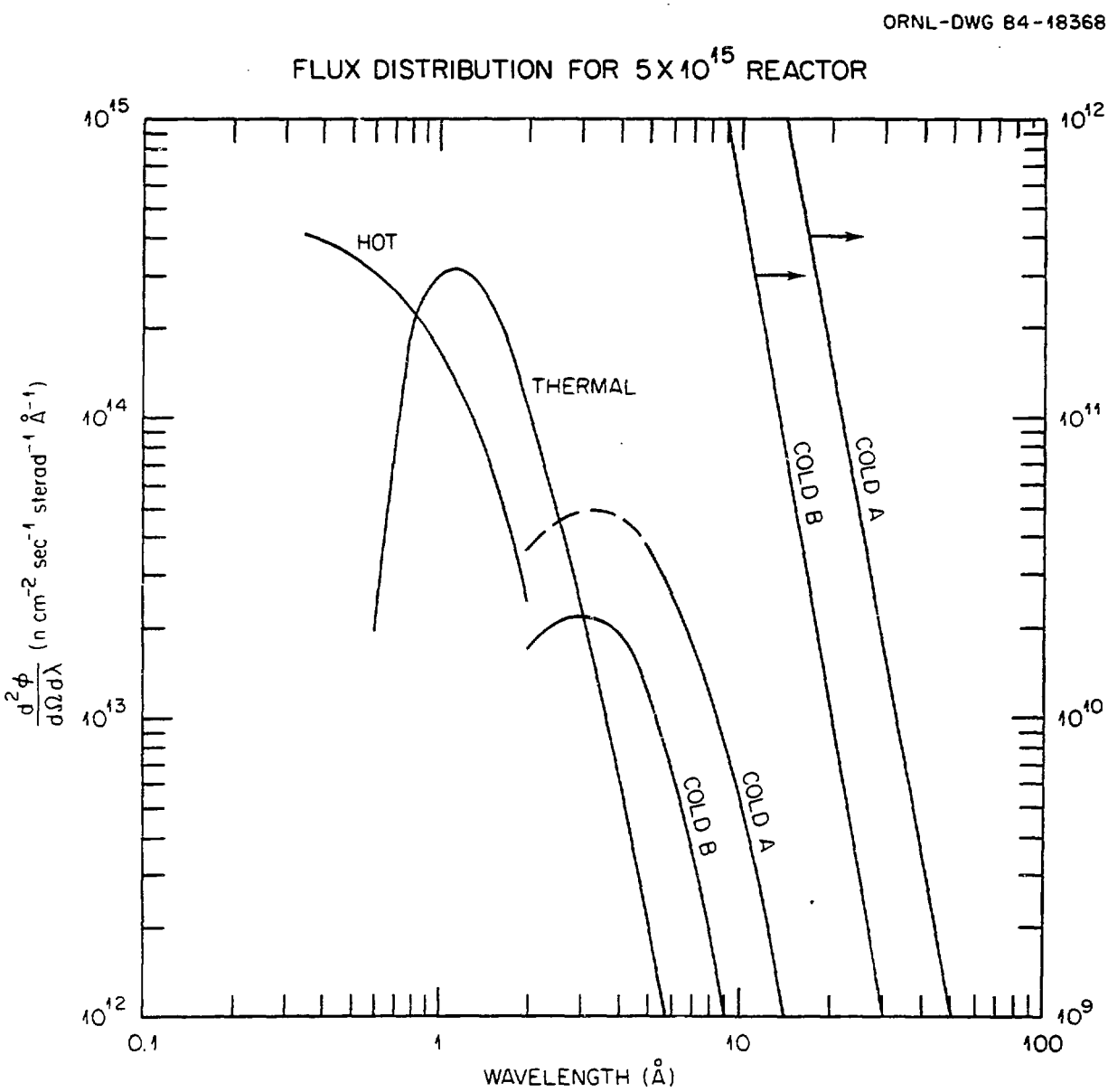
ORNL-DWG 84-18368
FLUX DISTRIBUTION FOR 5X10^15 REACTOR
HOT
THERMAL
COLD B
COLD A
COLD B
COLD A
10^15
10^14
10^13
10^12
10^12
10^11
10^10
10^9
0.1
1
10
100
WAVELENGTH (Å)
d²φ/dΩdλ (n cm⁻² sec⁻¹ sterad⁻¹ Å⁻¹)

Fig. 2

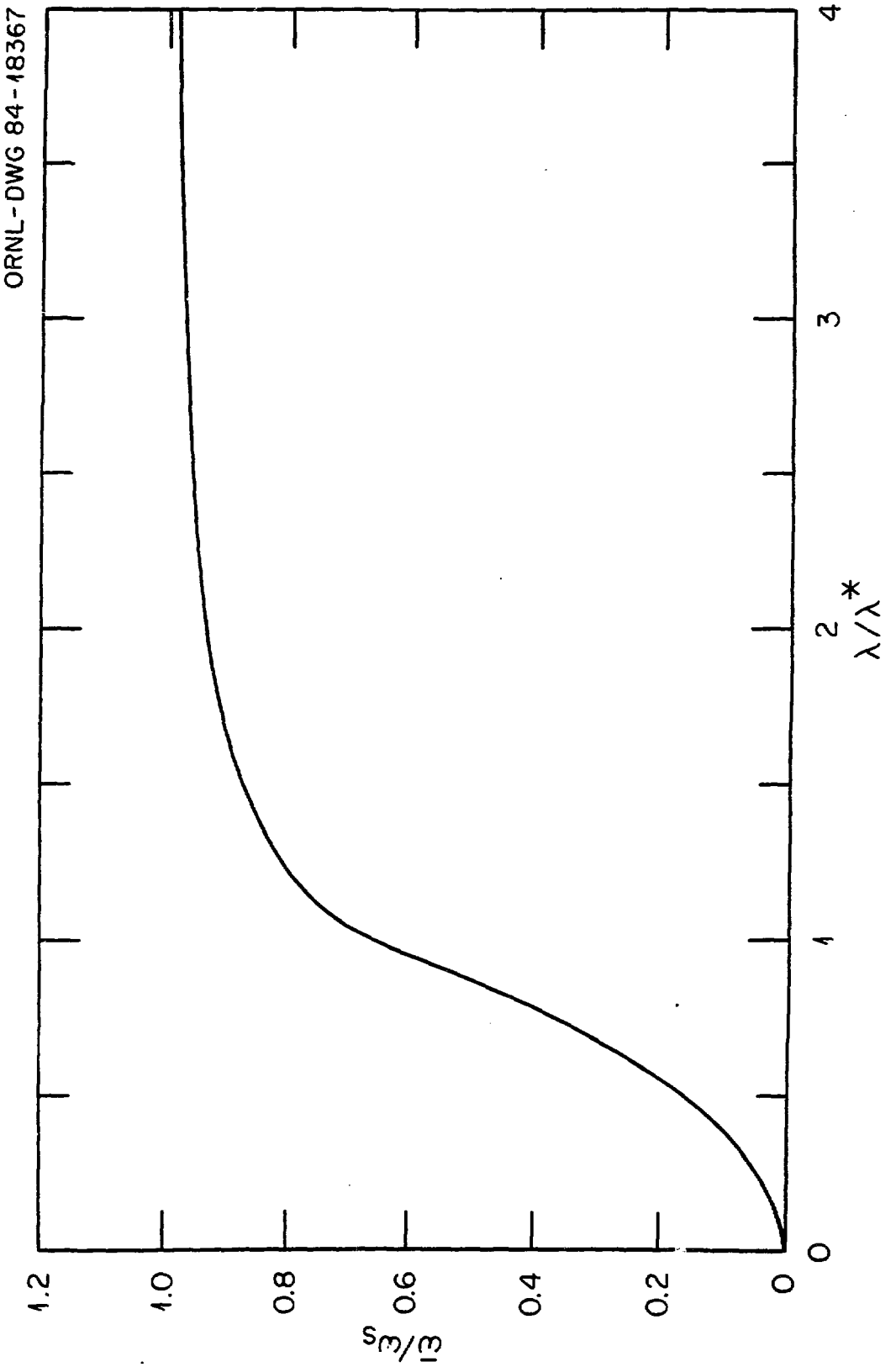
ORNL-DWG 84-18367
1.2
1.0
0.8
0.6
0.4
0.2
0
$\varepsilon/\varepsilon_s$
0
1
2
3
4
λ/λ^*

Fig. 3

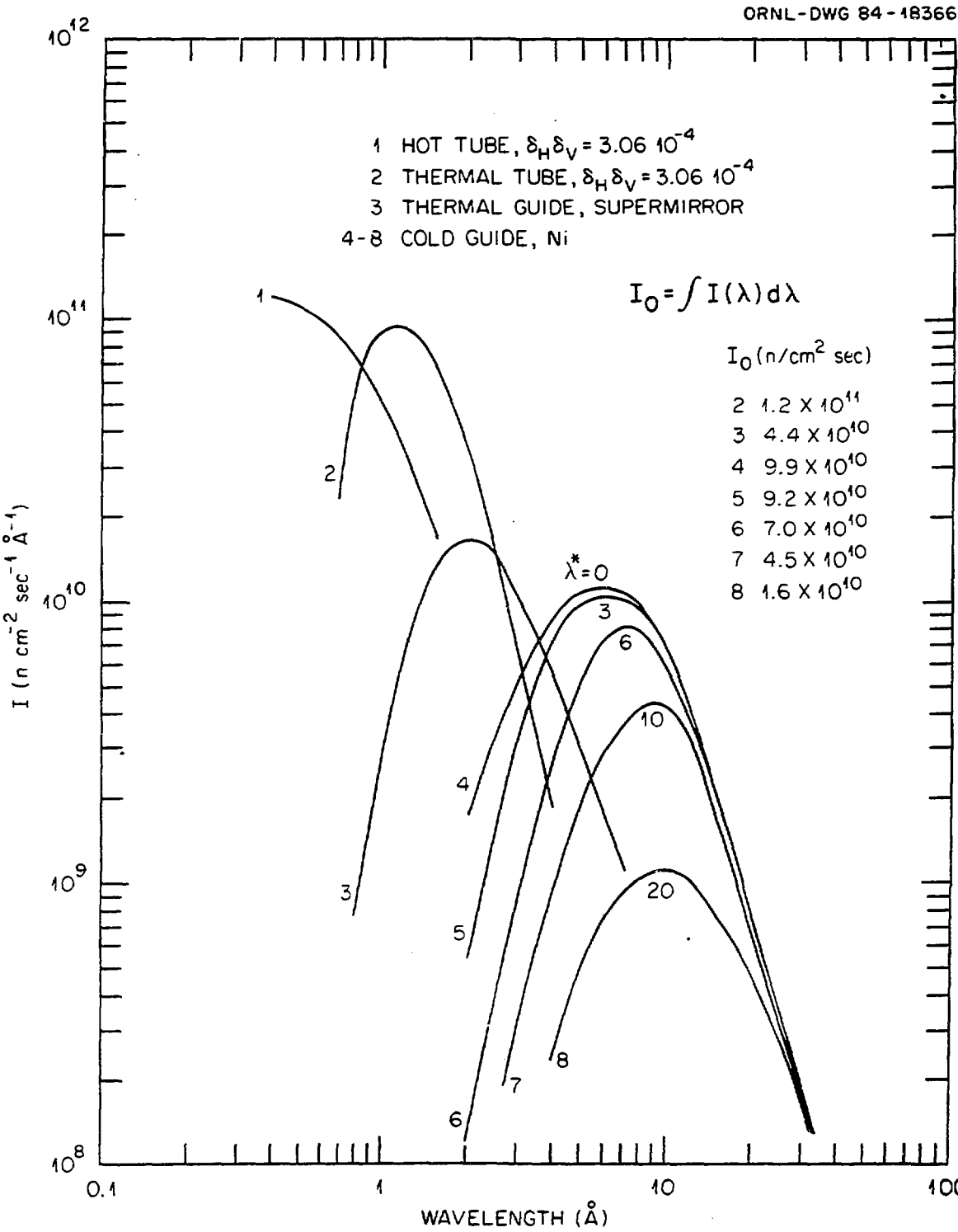
ORNL-DWG 84-18366
1 HOT TUBE, $\delta_H \delta_V = 3.06\ 10^{-4}$
2 THERMAL TUBE, $\delta_H \delta_V = 3.06\ 10^{-4}$
3 THERMAL GUIDE, SUPERMIRROR
4-8 COLD GUIDE, Ni
$I_0 = \int I(\lambda) d\lambda$
I_0 (n/cm^2 sec)
2 1.2×10^{11}
3 4.4×10^{10}
4 9.9×10^{10}
5 9.2×10^{10}
6 7.0×10^{10}
7 4.5×10^{10}
8 1.6×10^{10}
$\lambda^* = 0$
10^{12}
10^{11}
10^{10}
10^{9}
10^{8}
I (n cm^{-2} sec^{-1} Å^{-1})
0.1
1
10
100
WAVELENGTH (Å)

Fig. 4

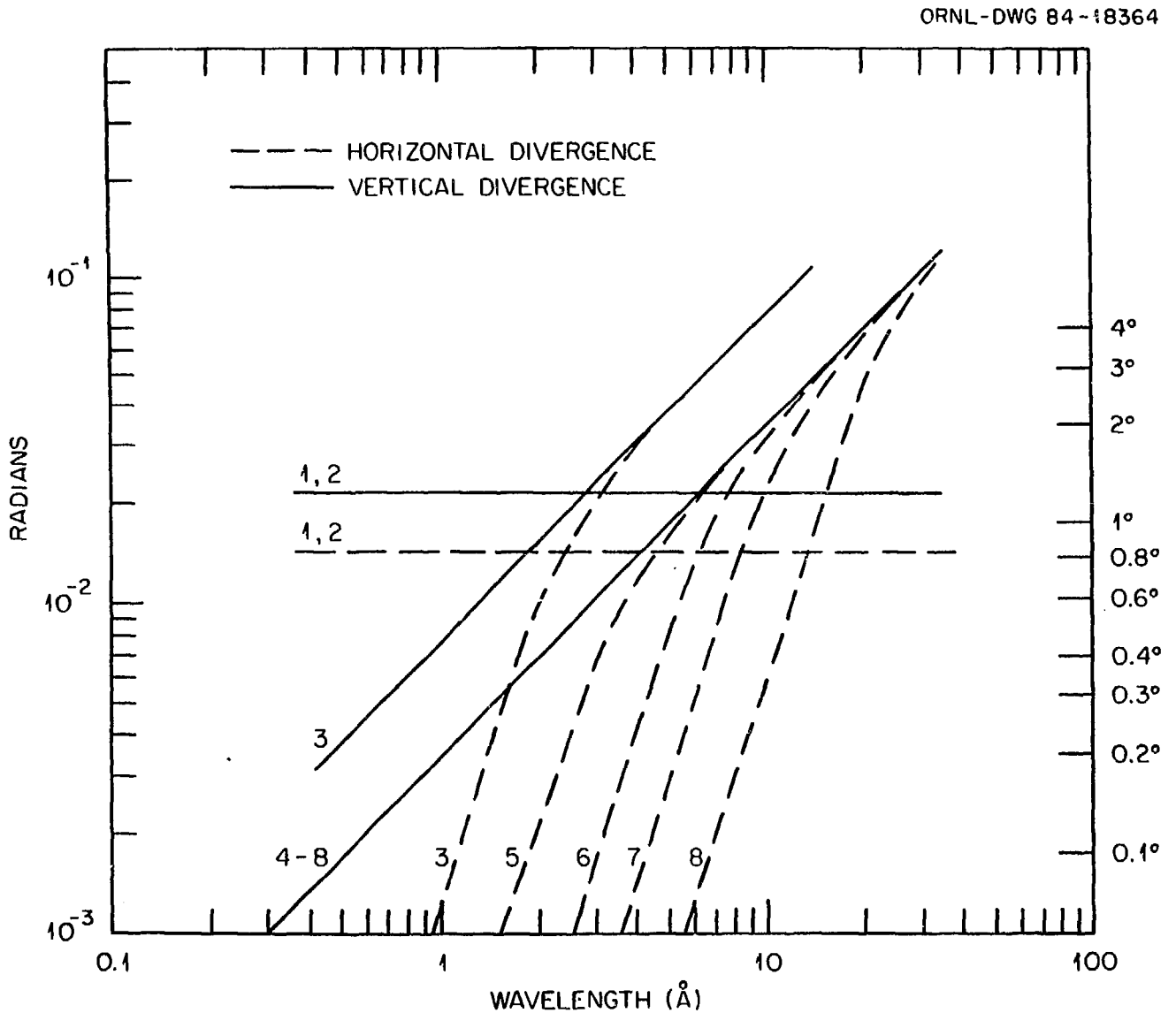
ORNL-DWG 84-18364
HORIZONTAL DIVERGENCE
VERTICAL DIVERGENCE
RADIANS
10^{-1}
10^{-2}
10^{-3}
1, 2
1, 2
3
4-8
3
5
6
7
8
4°
3°
2°
1°
0.8°
0.6°
0.4°
0.3°
0.2°
0.1°
0.1
1
10
100
WAVELENGTH (Å)

Fig. 5

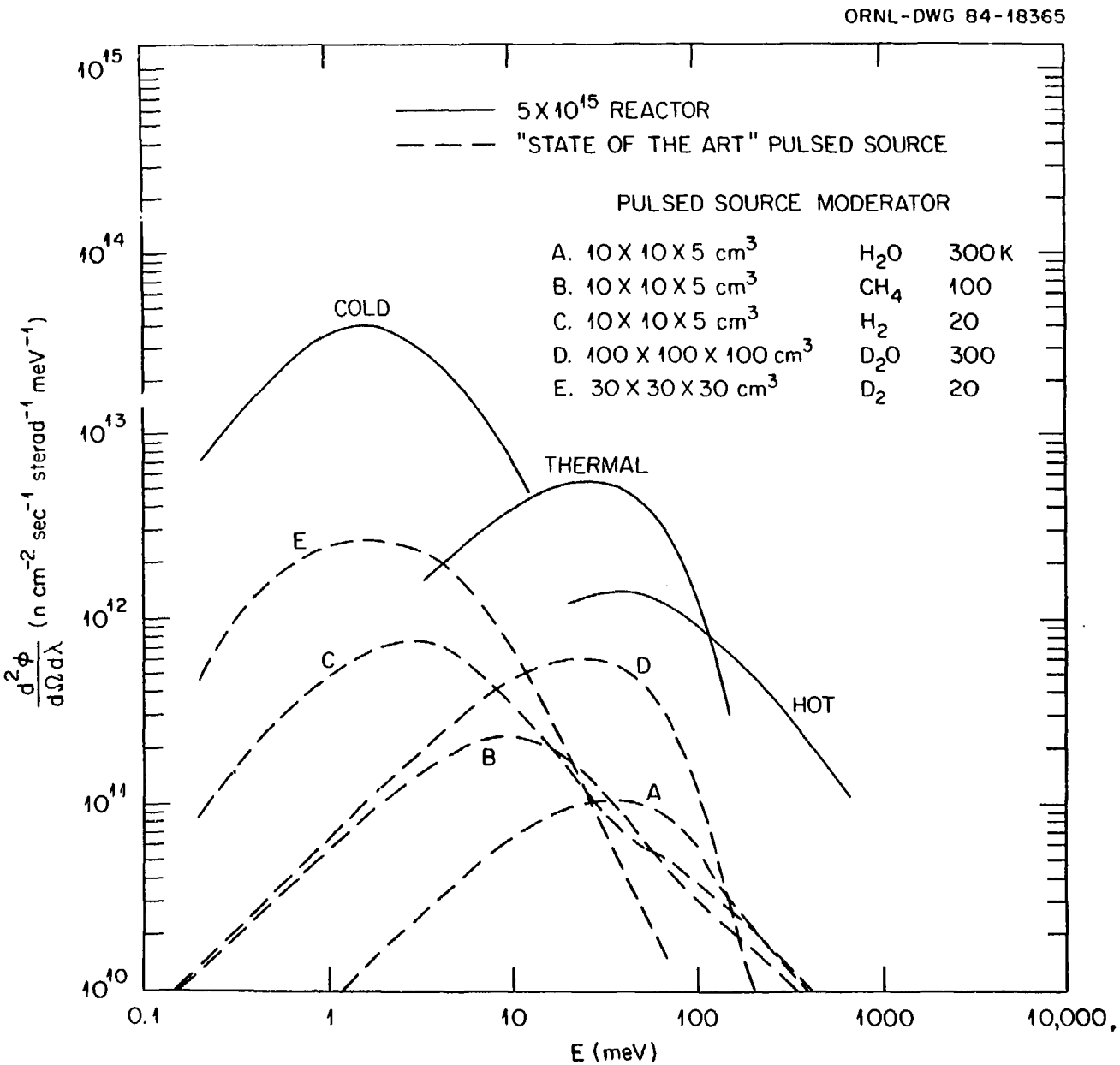
ORNL-DWG 84-18365
5X10^15 REACTOR
"STATE OF THE ART" PULSED SOURCE
PULSED SOURCE MODERATOR
A. 10 X 10 X 5 cm^3 H2O 300 K
B. 10 X 10 X 5 cm^3 CH4 100
C. 10 X 10 X 5 cm^3 H2 20
D. 100 X 100 X 100 cm^3 D2O 300
E. 30 X 30 X 30 cm^3 D2 20
COLD
THERMAL
HOT
E
C
D
B
A
d^2φ/dΩdλ (n cm^-2 sec^-1 sterad^-1 meV^-1)
E (meV)
10^15
10^14
10^13
10^12
10^11
10^10
0.1
1
10
100
1000
10,000.

Fig. 6